Neuroradiology (2013) 55:35–40
DOI 10.1007/s00234-012-1081-1

DIAGNOSTIC NEURORADIOLOGY

Three-dimensional susceptibility-weighted imaging at 7 T using fractal-based quantitative analysis to grade gliomas

Antonio Di Ieva · Sabine Göd · Günther Grabner · Fabio Grizzi · Camillo Sherif · Christian Matula · Manfred Tschabitscher · Siegfried Trattnig

Received: 14 April 2012 / Accepted: 27 July 2012 / Published online: 18 August 2012

Abstract
Introduction Susceptibility-weighted imaging (SWI) with high- and ultra-high-field magnetic resonance is a very helpful tool for evaluating brain gliomas and intratumoral structures, including microvasculature. Here, we test whether objective quantification of intratumoral SWI patterns by applying fractal analysis can offer reliable indexes capable of differentiating glial tumor grades.
Methods Thirty-six patients affected by brain gliomas (grades II–IV, according to the WHO classification system) underwent MRI at 7 T using a SWI protocol. All images were collected and analyzed by applying a computer-aided fractal image analysis, which applies the fractal dimension as a measure of geometrical complexity of intratumoral SWI patterns. The results were subsequently statistically correlated to the histopathological tumor grade.
Results The mean value of the fractal dimension of the intratumoral SWI patterns was 2.086±0.413. We found a trend of higher fractal dimension values in groups of higher histologic grade. The values ranged from a mean value of 1.682±0.278 for grade II gliomas to 2.247±0.358 for grade IV gliomas (p=0.013); there was an overall statistically significant difference between histopathological groups.
Conclusion The present study confirms that SWI at 7 T is a useful method for detecting intratumoral vascular architecture of brain gliomas and that SWI pattern quantification by means of fractal dimension offers a potential objective morphometric image biomarker of tumor grade.

The preliminary results of this study were presented at the 59th Congress of the Italian Society of Neurosurgery (SINch) in Milan, Italy; the Research Course of the European Association of Neurosurgical Societies (EANS) in Lausanne, Switzerland; and the 16th Congress of the Italian Society of Neurooncology (AINO) in Milan, Italy.

A. Di Ieva
Center for Anatomy and Cell Biology, Department of Systematic Anatomy, Medical University of Vienna,
Vienna, Austria

A. Di Ieva (✉)
Division of Neurosurgery, Department of Surgery, St. Michael's Hospital, University of Toronto,
30 Bond Street,
Toronto, ON M5B 1W8, Canada
e-mail: diieva@hotmail.com

S. Göd · G. Grabner · S. Trattnig
MR Centre of Excellence, Department of Radiology, Medical University of Vienna,
Vienna, Austria

F. Grizzi
IRCCS, Istituto Clinico Humanitas,
Rozzano, Milan, Italy

C. Sherif
Department of Neurosurgery, Krankenanstalt Rudolfstiftung,
Vienna, Austria

C. Matula
Department of Neurosurgery, Medical University of Vienna,
Vienna, Austria

M. Tschabitscher
Department of Anatomy,
Medical University of Brescia,
Brescia, Italy

Keywords Fractal dimension · Glioma · SWI · 7 T MRI

Abbreviations

FD Fractal dimension
FD_{SWI} Fractal dimension of the intratumoral SWI pattern
WHO World Health Organization

Introduction

It is well known that brain tumor growth and expansion are accompanied by the development of a unique microvascular bed [1]. Glioblastoma multiforme, the most aggressive glioma subtype [2], has highly heterogeneous histopathological features, including its microvascularity [3]. Neovascularization distinguishes grade III from grade IV brain tumors [2], and distinct neoplastic vascular patterns can offer information on patient prognosis [4, 5]. In clinical settings, it is compulsory to take advantage of parameters that can improve differential tumor diagnosis to assess the best treatment for the patient and improve survival [2]. While the current diagnostic gold standard is the histopathological interpretation of sampled tumor specimens [6], in vivo imaging techniques (e.g., MRI and/or nuclear medicine tools) are ideal modalities to assess glioma morphology, growth pattern, angiogenesis process, and metabolic profile in the preoperative setting [7].

In the last several years, susceptibility-weighted imaging (SWI) has been added to routine neuroimaging [8]. SWI is a method used to detect the magnetic susceptibility of different tissues [9] and is used to assess neoplastic microvasculature, microbleeds, and necrotic areas [10–14]. Although some qualitative or semiquantitative scoring systems have been proposed [15–18], an objective method to quantify intratumoral SWI patterns in ultra-high fields is still lacking.

The present study aimed to evaluate the potential of SWI pattern quantification by means of fractal analysis to differentiate glial brain tumor grades. The relevance of the study is the possible validation of an objective and computer-aided parameter (i.e., the fractal dimension of intratumoral SWI pattern at 7 T MRI, indicative of microangioarchitecture and microbleedings) as a potential morphometric image biomarker to estimate brain glial tumor grade in cancer research and in the clinic.

Materials and methods

Patients Thirty-six patients (19 females, 17 males) with glial brain tumor, as diagnosed with 3 T MRI, were retrospectively enrolled in the present study (Table 1). The mean age of the patients was 48±14.5 years (range, 20–78 years). The inclusion criteria of the patients were as follows: (a) age >18 years old and (b) no clinical contraindications to the neurosurgical resection of the tumor (as indicated by care providers) or to the execution of MR imaging. Patients underwent presurgical 7 T MRI (Magnetom 7T, Siemens Healthcare, Erlangen, Germany). The patients were informed of the potential side effects of ultra-high magnetic fields (including vertigo, nausea, loss of balance, claustrophobia, feelings of electric shocks, and skeletal muscle contractions) [19] before providing signed informed consent. The local ethics committee approved the study.

Table 1 Patients' characteristics

Patients' characteristics	Number
Number of patients	36
Gender, women/men	1:1.118
Median age (years), range	48, 20–78

Surgical procedure and neuropathology The patients underwent total or subtotal brain tumor resection at the Department of Neurosurgery of the Medical University of Vienna, Austria. Tumors were histologically evaluated by the local neuropathology team according to WHO 2007 criteria [2] as follows: 5 WHO grade II (2 astrocytomas, 3 oligodendrogliomas), 5 WHO grade III (4 astrocytomas, 1 oligoastrocytoma), and 22 WHO grade IV (glioblastoma multiforme) gliomas. Of the remaining four patients, the histological diagnosis and routine (3 T MRI) radiological findings did not allow an unequivocal classification (diffusely infiltrating gliomas with some rare findings of atypia, no gadolinium enhancement in neuroimaging) and were classified as grades II–III gliomas (four astrocytomas). Histological diagnosis divided the patients into four groups: grade II (n=5), grades II–III (n=4), grade III group (n=5), and grade IV (n=22) (Table 2).

7 T MRI T1-weighted data were acquired using a MPRAGE sequence (image matrix = 320×320, resolution = 0.76×0.72×0.7 mm, slices = 208, parallel imaging factor = 2, repetition time/inversion time/echo time = 3,800/1,700/3.55 ms, and acquisition time = 10.29 min). SWI data were acquired using three-dimensional, fully first-order flow-compensated gradient echo sequence (echo time = 15 ms at 7 T, repetition time = 28 ms, image matrix = 704×704 pixels, parallel imaging factor = 2, acquisition time =

Table 2 WHO grade and subtype

II (n=5)	II–III (n=4)	III (n=5)	IV (n=22)
Astrocytoma, 2 Oligodendroglioma, 3	Astrocytoma, 4	Astrocytoma, 4 Oligoastrocytoma, 1	GBM, 22

GBM glioblastoma multiforme

10.18 min, resolution = 0.3×0.3×1.2 mm). Eight-channel- (RAPID Biomedical; Würzburg, German) and 24-channel (Nova Medical, Wilmington, MA, USA) radiofrequency coils were used indifferently, with no differences in SWI image quality between the two coils. Two expert radiologists, who were blinded to the quantitative analysis, analyzed the images. The region of interest (ROI) (i.e., the tumor) was manually selected for each axial slice of the image stack that contained the tumor.

Post-processing and fractal analysis A physician, who was blinded to the radiological and histological results, applied fractal-based analysis to all selected ROIs of each patient to quantify the space-filling properties and the level of geometrical complexity of the intratumoral SWI signal, by means of the fractal dimension. The technical procedure of applying fractal analysis to 7 T SWI images has been extensively described elsewhere [20]. Briefly, all the images of the selected ROIs were analyzed using an ad hoc software tool developed in Visual C++ language for image and fractal analysis. Each image underwent auto-level filtering using the Brightness Progressive Normalization algorithm (http://www.fractal-lab.org/Downloads/bpn_algorithm.html) to achieve the same brightness and to use the same threshold in order to extract SWI patterns. Color segmentation was applied to select and extract black spots of the SWI patterns from the tumor. The space-filling properties (i.e., the geometrical complexity of the intratumoral SWI patterns) were quantified by means of the fractal dimension (FD_{SWI}), whose non-integer and nonlinear value is included in a 3D space, between 0 and 3 [21]. The box-counting method was used to assess the FD_{SWI} [20], and the statistical self-similarity of SWI patterns was found over 2 orders of magnitude in scale, as recognized for natural fractal objects [21]. The box-counting scaling window was ε_{min}=0.3–ε_{max}=3 mm.

Statistics The fractal analysis results of intratumoral SWI patterns were compared to the histopathological diagnosis to determine whether intratumoral microbleeds and microvasculature detected by SWI correlate with histopathological tumor grade. FD_{SWI} values were compared with histopathological findings using SPSS version 18.0 software (SPSS Inc., Chicago, IL, USA). Mann–Whitney *U* tests were used to compare the differences between groups, and *p* values <0.05 were considered statistically significant.

Results

The mean FD_{SWI} value of all cases was 2.086±0.413. Figure 1 shows the FD_{SWI} values for each group. A significant increasing trend ($p<0.05$) of FD_{SWI} was evident in higher grade groups: 1.682±0.278 (grade II), 1.790±0.227 (grades II–III), 2.018±0.517 (grade III), 2,247±0.358 (grade IV), as schematically shown in Fig. 2. The strongest statistical significance was found between grade II and grade IV ($p=0.013$). In addition, when grade II gliomas were considered "lower grade gliomas" ($n=5$) and grades II–III, III, and IV ($n=31$) were "higher grade gliomas", the difference between the two groups remained statistically significant ($p=0.016$) (Fig. 3, left). Excluding the four "ambiguous" cases (groups II–III)

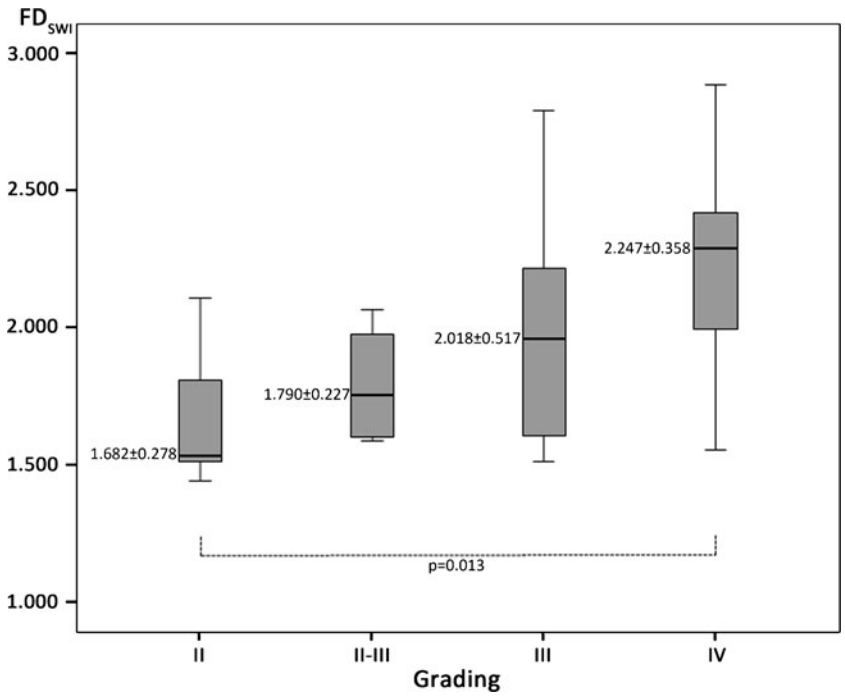

Fig. 1 Box plots showing FD_{SWI} values for each histopathological group of gliomas (overall statistically significant difference, $p<0.05$). The strongest statistical significance was found in the grade II gliomas versus grade IV group

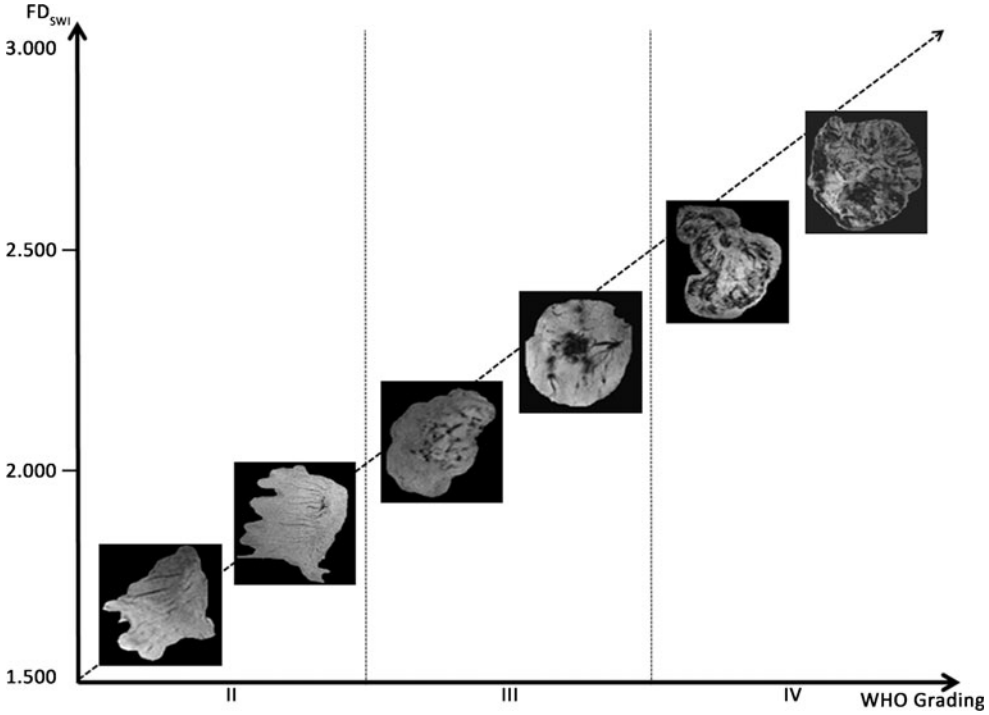

Fig. 2 Schema showing the trend of higher FD_{SWI} values in groups of higher histopathological tumor grades. The intralesional SWI patterns consist of distinct vascular structures (linear structures in grade II tumors, increasing in tortuosity and density in higher grades gliomas) and conglomerated dot shapes, which most likely indicate intralesional bleeding and/or necrotic areas (as evident in grades III and IV gliomas). It should be noted that the images in the schema are only selections of the whole stack of axial sections of the tumor. However, the fractal dimension was measured with the volume of the three-dimensional reconstruction of the whole tumor

and analyzing the lower grade glioma group (grade II, $n=5$) versus the higher grade glioma group (grades III and IV groups together, $n=27$), the difference was also significant ($p=0.01$) (Fig. 3, right). The comparison of grade III versus grade IV gliomas did not yield a significant result ($p=0.692$). Not surprisingly, there was no statistical significance when the histological grades II–III glioma group was considered alone versus the grade II group and versus the higher grade groups, confirming that this tumor group has heterogeneous structural features that are incompatible with unequivocal grading.

Discussion

SWI sequences provide information on venous vasculature, hemorrhage, iron deposits [11–13], and very small vascular structures within the central nervous system (including brain tumors), especially when performed at ultra-high fields [14, 17, 22–28]. Lower field (1.5 T) SWI is sensitive to intratumoral microbleeds and is useful in glioma grading [29, 30]. Zhang et al. quantified SWI spots by frequency and maximum diameter [30]. However, the relatively low-

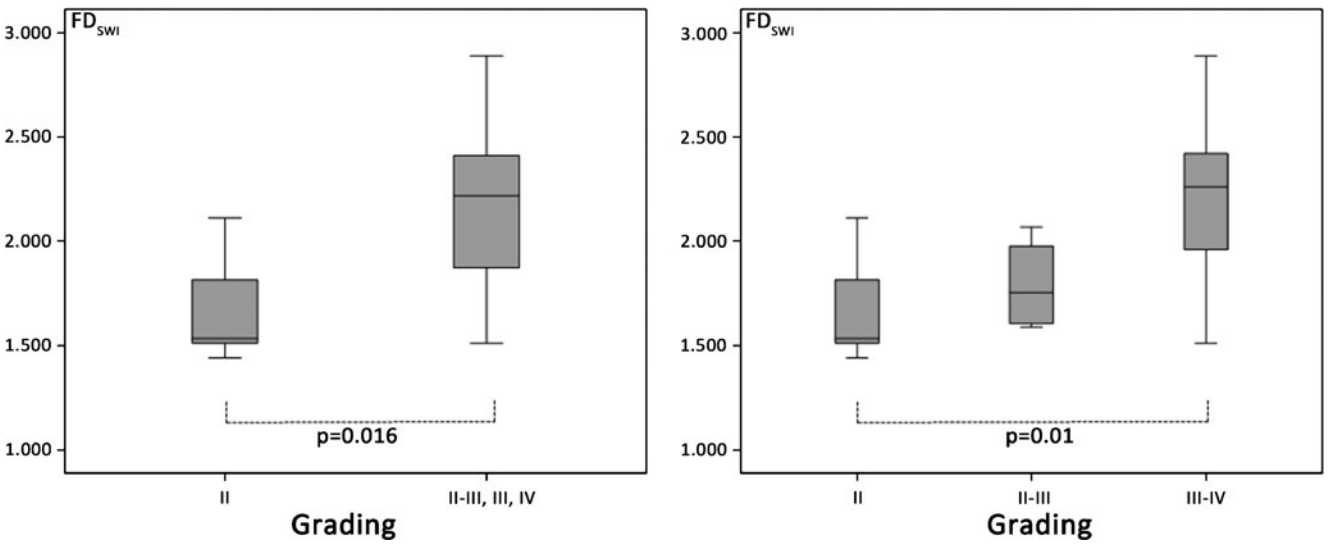

Fig. 3 Box plots of low-grade gliomas (grade II, $n=5$) versus higher grade gliomas (grades II–III, III, and IV, $n=31$) (*left*). On the *right*, comparison of the groups with exclusion of the four "ambiguous" cases (groups II–III)

magnetic field used did not offer sufficient spatial resolution to detect intratumoral vasculature. Hori et al. proposed a semiquantitative scoring system to quantify intratumoral SWI hypointensity at 1.5 and 3 T and to differentiate brain gliomas grades [16, 17]. It is our opinion that this scoring system is affected by potential intra- and inter-observer variability, similarly to all semiquantitative methods in which the operators (radiologists or pathologists) subjectively assign a score.

Fractal geometry has been demonstrated to offer appropriate tools to quantify irregular-shaped biological objects, including microvascular patterns [31]. The microvascular fractal dimension has been shown as a reliable numerical index to objectively quantify geometrical complexity of microvascular patterns in brain tumors [31]. The fractal dimension is a characteristic of irregularly shaped structures that maintains a constant level of complexity over a limited range of scales [21]. The higher signal-to-noise ratio, higher spatial resolution, and increased phase differences offered by 7 T MRI compared with the 3 T MRI, as well as the objective quantification of SWI patterns by means of fractal analysis, are valid tools to improve preoperative differential diagnosis of brain gliomas. The methods for applying fractal analysis in quantifying intratumoral SWI patterns in 7 T MRI have been described previously, suggesting the use of FD_{SWI} as a potential and reliable biomarker for the follow-up of patients undergoing antiangiogenic treatment [20]. Ultra-high-field imaging has provided in vivo information for identifying distinct "fingerprints" in rodent glioma models [32], and fractal analysis seems to be the most reliable and quantitative approach for objectively describing such findings. Our results show that lower FD_{SWI} values are associated with tumoral microvasculature, while higher values (more "space-filling" and geometrically complex) are associated with microbleeds and necrotic areas (Fig. 2), as previously indicated in qualitative [27], semiquantitative [17], and quantitative [20] studies. These speculations could be definitively confirmed by direct comparisons between local SWI patterns in MRI and the specific tissue specimens. Moreover, fractal analysis of SWI neoplastic patterns could be integrated with other neuroradiological parameters (e.g., histogram analysis of diffusion tensor imaging-derived maps) [33] to achieve new information about tumor biology that would assist in determining patient treatment and prognosis.

The present study has limitations. First, there are some limits regarding the quantification of SWI patterns, specifically understanding the source of the SWI signal: the intratumoral SWI patterns most likely correspond to pathological intratumoral microvasculature [14], even though high heterogeneity of the structures giving rise to the signal (i.e., iron deposits, necrotic areas and microbleeds) led us to call it "SWI pattern" and not "microvascular pattern". In addition, the image analysis is based on the subjective choice of ROIs by a neuroradiologist. Even if this is a routine radiologic procedure, it introduces intra- and inter-observer variability. Therefore, although fractal analysis is more appropriate in analyzing irregular-shaped forms and heterogeneous patterns and is applied by an objective computer-aided procedure, the ROIs choice might be biased. Applying different methods to estimate fractal dimension can give different results, so standardized protocols should be employed [31]. We used the box-counting method because it is the most used algorithm to assess fractal dimensions of natural objects in biomedical research, even if several different techniques have been described [21]. This underscores the necessity of standardizing methodological techniques so that obtained numerical results can be compared. It should also be emphasized that fractal geometry is a mathematical approach with intrinsic limitations, especially when applied to natural objects that are not ideal mathematical fractals. However, our findings suggest that higher FD_{SWI} values correspond to higher geometrical complexity of intratumoral structures and seem to correlate with higher grades of glial tumor malignancy. Our methodology could be a reliable tool in the neuroradiological armamentarium for the diagnosis and follow-up of brain tumor patients.

Conclusion

In conclusion, we found a significant association between FD_{SWI} values and histological grade of glial brain tumors, suggesting that the combined use of 7 T SWI imaging and fractal analysis allows differentiation of histopathological grades. This research should stimulate further studies to determine objective, quantitative neuroimaging measurements to be used in differential brain tumor diagnosis. Here, we showed that there is a gradient in SWI pattern values that corresponds to geometrical complexity from low- to high-grade brain glial tumors. Due to the small numbers of patients, these data should be supported by further studies to verify the existence of specific structural and microvascular patterns in distinctly graded brain tumors. Fractal analysis should be considered a useful tool to quantify microvascular networks in pathology as well as in radiology. The fractal dimension of intratumoral SWI patterns deserves further investigation as a potential image biomarker to analyze intrinsic neoplastic architecture, improve clinical neuroimaging differential tumor diagnosis, determine appropriate therapy, and improve patient prognosis and survival.

Acknowledgments ADI received a 2010 research grant from the Italian Society of Neurosurgery (SINch) and a 2011 Aesculap European Association of Neurosurgical Societies Laboratory Research Prize. This study was supported by the Jubiläumsfonds of the Austrian National Bank (grant no. 13457). The authors wish to thank FMEA (the Society for the Promotion of Research in Microsurgical and Endoscopic Anatomy) for funding the production of this article. We would like to give special thanks to the *Virtual Fractal Lab* Team (www.fractal-lab.org) for developing the software used here and for their continued technical support beyond image and fractal analyses.

Conflict of interest We declare that we have no conflict of interest.

References

1. Jain RK et al (2007) Angiogenesis in brain tumors. Nat Rev Neurosci 8:610–622
2. Louis DN et al (2007) The 2007 WHO classification of tumours of the central nervous system. Acta Neuropathol 114:97–109
3. Di Ieva A et al (2011) Angioarchitectural heterogeneity in human glioblastoma multiforme: a fractal-based histopathological assessment. Microvasc Res 81:222–230
4. Folkert RD (2000) Descriptive analysis and quantification of angiogenesis in human brain tumors. J Neurooncol 50:165–172
5. Birner P et al (2003) Vascular patterns in glioblastoma influence clinical outcome and associate with variable expression of angiogenic proteins: evidence for distinct angiogenic subtypes. Brain Pathol 13:133–143
6. Van den Bent MJ (2010) Intraobserver variation of the histopathological diagnosis in clinical trials on gliomas: a clinician's perspective. Acta Neuropathol 120:297–304
7. Essig M et al (2011) MR imaging of neoplastic central nervous system lesions: review and recommendations for current practice. AJNR Am J Neuroradiol. doi:10.3174/ajnr.A2640
8. Robinson RJ, Bhuta S (2011) Susceptibility-weighted imaging of the brain: current utility and potential applications. J Neuroimaging 21:189–204
9. Haacke EM et al (2004) Susceptibility weighted imaging (SWI). Magn Reson Med 52:612–618
10. Li C et al (2009) Susceptibility-weighted imaging in grading brain astrocytomas. Eur J Radiol 75:87–95
11. Rauscher A et al (2005) Magnetic susceptibility-weighted MR phase imaging of the human brain. AJNR Am J Neuroradiol 26:737–742
12. Rauscher A et al (2005) High resolution susceptibility weighted MR-imaging of brain tumors during the application of a gaseous agent. Rofo 177:1065–1069
13. Rauscher A et al (2005) Noninvasive assessment of vascular architecture and function during modulated blood oxygenation using susceptibility weighted magnetic resonance imaging. Magn Reson Med 54:87–95
14. Moenninghoff C et al (2010) Imaging of adult astrocytic brain tumors with 7T MRI: preliminary results. Eur Radiol 20:704–713
15. Pinker K et al (2007) High-resolution contrast-enhanced, susceptibility-weighted MR imaging at 3 T in patients with brain tumors: correlation with positron-emission tomography and histopathologic findings. AJNR Am J Neuroradiol 28:1280–1286
16. Hori M et al (2010) Precontrast and postcontrast susceptibility-weighted imaging in the assessment of intracranial brain neoplasms at 1.5 T. Jpn J Radiol 28:299–304
17. Hori M et al (2010) Three-dimensional susceptibility-weighted imaging at 3T using various image analysis methods in the estimation of grading intracranial gliomas. Magn Reson Med 28:594–598
18. Kim HS et al (2009) Added value and diagnostic performance of intratumoral susceptibility signals in the differential diagnosis of solitary enhancing brain lesions: preliminary study. AJNR Am J Neuroradiol 30:1574–1579
19. Theysohn JM et al (2008) Subjective acceptance of 7 Tesla MRI for human imaging. MAGMA 21:63–72
20. Di Ieva A et al (2012) Fractal analysis of the susceptibility weighted imaging patterns in malignant brain tumors during antiangiogenic treatment: technical report on four cases serially imaged by 7 T magnetic resonance during a period of four weeks. World Neurosurg. doi:10.1016/jwneu.2011.09.006
21. Losa GA (2009) The fractal geometry of life. Riv Biol 102:29–59
22. Cho ZH et al (2008) Observation of the lenticulostriate arteries in the human brain in vivo using 7.0 T MR angiography. Stroke 39:1604–1606
23. Conijn MM et al (2009) Perforating arteries originating from the posterior communicating artery: a 7.0-Tesla MRI study. Eur Radiol 19:2986–2992
24. Lupo JM et al (2009) GRAPPA-based susceptibility-weighted imaging of normal volunteers and patients with brain tumor at 7 T. Magn Reson Imaging 27:480–488
25. von Morze C et al (2007) Intracranial time-of-flight MR angiography at 7 T with comparisons to 3 T. J Mag Reson Imaging 26:900–904
26. Di Ieva A et al (2011) The veins of the nucleus dentatus: anatomical and radiological findings. NeuroImage 54:74–79
27. Grabner G et al (2012) Longitudinal brain imaging of five malignant glioma patients treated with bevacizumab using susceptibility-weighted magnetic resonance imaging at 7 T. Magn Reson Imaging 30:139–147
28. Moser E et al (2012) T MR-from research to clinical applications? NMR Biomed 25:695–716
29. Sehgal V et al (2006) Susceptibility-weighted imaging to visualize blood products and improve tumor contrast in the study of brain masses. J Magn Reson Imaging 24:41–51
30. Zhang W et al (2010) Application of susceptibility weighted imaging in revealing intratumoral blood products and grading gliomas. J Radiol 91:485–490
31. Di Ieva A (2010) Angioarchitectural morphometrics of brain tumors: are there any potential histopathological biomarkers? Microvasc Res 80:522–533
32. Doblas S et al (2010) Glioma morphology and tumor-induced vascular alterations revealed in 7 rodent glioma models by in vivo magnetic resonance imaging and angiography. J Mag Reson Imaging 32:267–275
33. Jakab A et al (2011) Glioma grade assessment by using histogram analysis of diffusion tensor imaging-derived maps. Neuroradiology 53:483–491